Gas-solids kinetics of CuO/Al2O3 as an oxygen carrier for high-pressure chemical looping processes : the influence of the total pressure

Please check the document version of this publication:

• A submitted manuscript is the version of the article upon submission and before peer-review. There can be important differences between the submitted version and the official published version of record. People interested in the research are advised to contact the author for the final version of the publication, or visit the DOI to the publisher's website.
• The final author version and the galley proof are versions of the publication after peer review.
• The final published version features the final layout of the paper including the volume, issue and page numbers.
Link to publication

Download date: 16. Nov. 2023

Gas-solids kinetics of CuO/Al$_2$O$_3$ as an oxygen carrier for high-pressure chemical looping processes: the influence of the total pressure

M.A. San Pio, F. Gallucci*, I. Roghair, M. van Sint Annaland

Chemical Process Intensification, Department of Chemical Engineering and Chemistry, Eindhoven University of Technology, P.O. Box 513, 5600 MB Eindhoven, The Netherlands.

Abstract

Copper oxide on alumina is often used as oxygen carrier for chemical looping combustion owing to its very high reduction rates at lower temperatures and its very good mechanical and chemical stability at not too high temperatures. In this work, the redox kinetics of CuO/Al$_2$O$_3$ have been studied at elevated pressures and temperatures. All the experiments have been started under the same initial conditions to assure the same starting point. While other studies reported a negative effect of the total pressure on the redox kinetics, this study shows that this negative effect of the pressure is most probably caused by external mass transfer limitations in previous studies. Additionally, as long as external mass transfer limitations are prevented, the total pressure at which the reduction is performed does not affect the redox kinetics nor the morphological and chemical structure of the oxygen carrier. The sudden decrease in the reduction rate at higher particle conversions was not influenced by the operating pressure and was attributed to limitations in the spinel reduction kinetics.

Keywords

Corresponding author

(*) E-mail: F.Gallucci@tue.nl

1 Introduction

The long term solution to mitigate climate change caused by human activities requires the replacement of fossil fuels by sustainable resources. On the midterm, however, while the transition to renewable resources is taking place, fossil fuels will still play an important role in the energy conversion processes, so that the effects on the climate can only be combatted by decreasing the anthropogenic CO_2 emissions related to fossil fuel combustion. This can be achieved by integration of carbon capture and storage (CCS) in the power production and energy intensive processes [1]. Separation (capture) of CO_2 can be achieved through a number of different technologies, often resulting however in large energy penalties [2–8]. The chemical-looping combustion (CLC) process is a very interesting new technology, in which the separation of CO_2 is integrated with the power production process by avoiding direct contact between the fuel and air, and thereby the dilution of the CO_2 rich stream with N_2. The fuel is combusted in the fuel reactor with an oxygen carrier (a supported metal oxide) producing a CO_2/H_2O mixture, while the oxygen carrier is reduced. The oxygen carrier is subsequently oxidized to its original state with air in the air reactor. The use of a pressurized CLC (15 bar or higher) and high temperature (1000-1200 °C) [9] is especially competitive compared with other capture technologies and with low pressure CLC. First, the efficiency of the cycle in the CLC power plant will be increased (energy penalty in the order of 2%) [10]; second, the CO_2 recovery as a high-pressure gas requires only a relatively small amount of additional power for further compression of the CO_2 stream to pipeline (35 bar) or sequestration pressures (100 bar) [8]. In view of the efficiency gains by operation at elevated pressures, particularly dynamically operated packed bed CLC reactors [11], where the oxygen carrier is stationary and is alternately reduced and oxidized via periodic switching of the fuel and air streams, show promise because of their

relative ease of operation at higher pressures, in comparison to interconnected fluidized bed reactor systems [12].

Oxygen carriers are one of the most important elements of the CLC technology, as they determine to a large extent the overall process efficiency. Therefore, accurate knowledge of the redox kinetics is extremely important for the modelling and design of chemical looping processes, and in particular for packed-bed CLC processes, where the oxygen carrier particle are operated with a large difference between the reduction and oxidation states. Most power plant integration studies with CLC assume that the process is operated at elevated pressures, but there is lack of knowledge on the reactivity of the oxygen carriers at elevated pressures.

Several authors have observed the negative effect of increasing the total pressure on the gas-solid reaction rates and have proposed different explanations. Chauk et al. [13] have studied the effect of the total pressure and H_2S partial pressure on the extent of sulfur capture and sorbent conversions. They showed with experiments where the partial pressure of H_2S was kept constant while changing the total pressure, there was a negative effect on the combined calcination and sulfidation steps. They observed a change in the structural properties, and proposed this as a possible explanation of the adverse effect of the total pressure on the redox kinetics. They also studied the influence of the partial pressure of H_2S while keeping the total pressure constant, observing that the sulfidation rate of CaO increases with increasing H_2S partial pressure. Agnihotri et al. [14] proposed that the increase of moles of gas produced during the sulfidation of Ca-based sorbents was responsible for the negative pressure effect. Qui and Lindqvist [15] observed that the kinetic rate constant and the effective diffusivity of SO_2 through the product layer decreased as the total pressure increased. Qui et al. [16] explained the negative effect of the total pressure on the kinetics by the inhibition of gas diffusion in the porous particles. Garcia

Labiano et al. [17] studied the effect of the pressure on the reactivity of copper, iron and nickel based oxygen carriers, reporting a negative effect of the total pressure on the kinetics. They developed a model using a dependency on total pressure of the effective diffusivity in the pores and in the product layer to predict their experimental results [18].

All these authors [14–16,18–20] have reported that the pressure has a surprisingly negative effect on the reactivity of the solids. Despite the importance of this effect, there is no general conclusion and no physical explanation on the cause for the observed negative influence of the pressure on the kinetics.

Supported copper-based oxygen carriers have been proposed as interesting oxygen carriers for CLC processes, and in particular as the preferred oxygen carrier of the first bed in the two-stage packed bed CLC process, especially because of their high reduction rates at relatively low temperatures and its very good mechanical and chemical stability at not too high temperatures [21]. The kinetics of the Cu/CuO oxidation/reduction at low pressure are often described with a combination of reactions occurring in series and parallel [22–26]. In this work the redox kinetics of a CuO/Al_2O_3 oxygen carrier has been studied under different operating pressures keeping the partial pressure of the reducing/oxidizing gas constant in order to better understand the pressure effect on the redox kinetics of the oxygen carriers and to elucidate the reason for the often observed negative effect of the total pressure on the redox kinetics. The objectives of this paper are: (i) to investigate the effect of the total pressure on the redox kinetics, ii) to study the morphological changes at different pressures, and iii) to explain the observed reaction rates at different pressures and temperatures.

After a description of the experimental techniques used in this work, the results of the different experiments on the CuO/Al$_2$O$_3$ oxygen carrier over many consecutive redox cycles at different pressures are presented and discussed. XRD has been used to characterize the oxygen carrier and to investigate whether the interactions between the metal oxide and the support play a role when operating at different pressures. Determination of the BET surface areas is used to study if the surface area changes with operation at elevated pressures and SEM is used to observe the change in internal morphology as a function of operation pressure.

2 Material and Methods

2.1 Effect of pressure on CuO/Al$_2$O$_3$ kinetics

The experiments have been carried out in three different thermogravimetric analysers (TGAs) with a 12.5 wt% CuO/Al$_2$O$_3$ (1.1 mm diameter - Sigma-Aldrich) oxygen carrier to measure the redox kinetics. Three TGAs were used in this work to assure that the measured kinetics are not due to an effect of the TGA but reproducible in other systems. The reactivity of all the experiments described in this work in all the TGAs have been carried out using consecutive redox cycles starting always from the same material state. This has been obtained by carrying out three redox cycles at 1000 °C and atmospheric pressure and 50% H$_2$, 50% N$_2$ as reducing gas prior to every experiment (with short intermediate N$_2$ purges), as described in more detail in [24]. The reduction cycles were carried out using H$_2$ and N$_2$ during the reduction, with different concentrations to keep the partial pressure of H$_2$ constant to 1 bar, and air during the oxidation cycles, at different temperatures ranging from 600 °C to 1000 °C and different total pressures ranging from 1 to 10 bar. A redox cycle consists of 15 min reduction and 10 min oxidation with two minutes purge (with nitrogen) between the reduction and oxidation cycles to avoid mixing of the different reactants. The N$_2$ and H$_2$ used in these experiments have a 99.999% purity (with

$O_2 < 4$ ppm), and 99.9999% (with $O_2 < 0.5$ ppm), respectively, according to the specifications (Linde gas).

Blank measurements were performed for each experiment in all the TGAs used in this work, under the same conditions, using the empty basket to correct the balance signal for density changes in the reactor caused by changes in the feed gas (e.g. N_2 compared to H_2) and reactor temperature. At higher pressures, the blank correction becomes more important due to buoyancy effects [27].

The oxygen carrier conversion (X_s) is subsequently calculated from the observed mass change in the oxygen carrier under different experimental conditions, defined by Eq. (1),

$$X_s = \frac{m - m_{red}}{m_{ox} - m_{red}} \qquad (1)$$

where m is the current mass and m_{ox} and m_{red} are the mass of the fully oxidized and reduced forms of the oxygen carrier. The fully oxidized mass is taken as the mass of the fresh material which was delivered in oxidized form.

2.1.1 Magnetic suspension balance

The magnetic suspension balance is a thermogravimetric analyser from Rubotherm (MSB) that works at high pressures up to 30 bar (denoted as HPTGA (High Pressure TGA). Themass change is measured, while the reactant concentration, temperature or pressure is varied. In this setup, the solid sample (typically 100 mg) is placed in a quartz glass sample holder, which is connected to a balance with an Ir wire connected to the permanent magnet. The operating conditions can vary between 1 and 30 bar and 20-1200 °C. Air, H_2, CO, CO_2, CH_4 and steam can be fed as reactants. Gas flow rates are controlled by Mass Flow Controllers (Bronkhorst) with the total gas flow rate

set at 480 mL/min [28]. The reactant gases are supplied at the top of the reactor. The reactor is surrounded by a vessel that is maintained at lower temperature. Argon is supplied to this vessel to prevent that reactant gases can enter and mix in the insulation layer. A schematic representation of the setup can be found in Fig.1.

Before a series of experiments is started, the system is pressurized and the reactor is set at the desired operating temperature. When this temperature is reached and the system has been stabilized, redox cycles are carried out that consist of 15 min reduction, 2 min purge and 10 min oxidation.
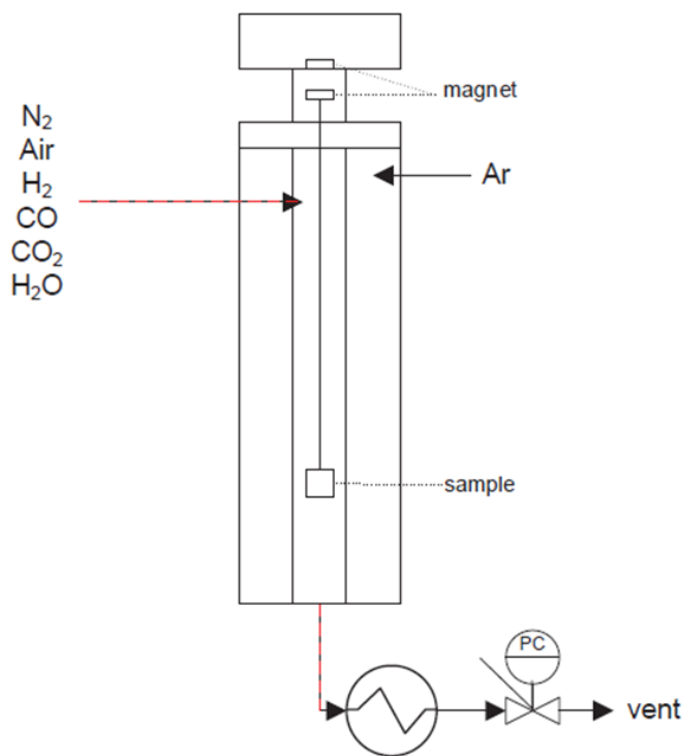

Fig.1. Schematic overview of the magnetic suspension balance (HPTGA) used in this work (PC = pressure controller).

2.1.2 Thermogravimetric analyser at low pressure

This thermogravimetric analyser works at atmospheric pressure (denoted as LPTGA (Low Pressure TGA) and it is used to measure and analyze the oxygen carrier reactivity at different flow rates in order to assure that no mass transfer limitations play a role. The LPTGA consists of a cylindrical quartz reactor (15 mm i.d.) placed in an oven that can be operated at up to 1200 °C and atmospheric pressure. For a schematic representation of this setup the reader is referred to [29]. A sample (typically about 100 mg) is placed in a quartz sample-holder (40 μm pore size) connected to a CI Precision microbalance with a platinum wire. The temperature and weight of the sample are continuously monitored, while the gas flow rates are controlled by Mass Flow Controllers (Bronkhorst).

2.1.3 High-Pressure Thermogravimetric-Analyser High Flow

TGA experiments at high pressure were carried out in a similar in-house designed setup for operation up to 10 bar (denoted as HP_ TGA_HF (High Pressure High Flow TGA). A microbalance (Sartorius MD25) with a sensitivity of 1 μg and 200 mg of operating range connected to a reactor allowed for TGA experiments up to 10 bar [27]. The maximum temperature of this reactor is 1100 °C. A porous quartz basket or a porous ceramic basket was used which contained typically 100 mg of catalyst. A schematic representation is shown in Fig. 2. The TGA was modified in order to be able to feed up to 6 L/min of N_2 in order to assess the influence of mass transfer limitations.
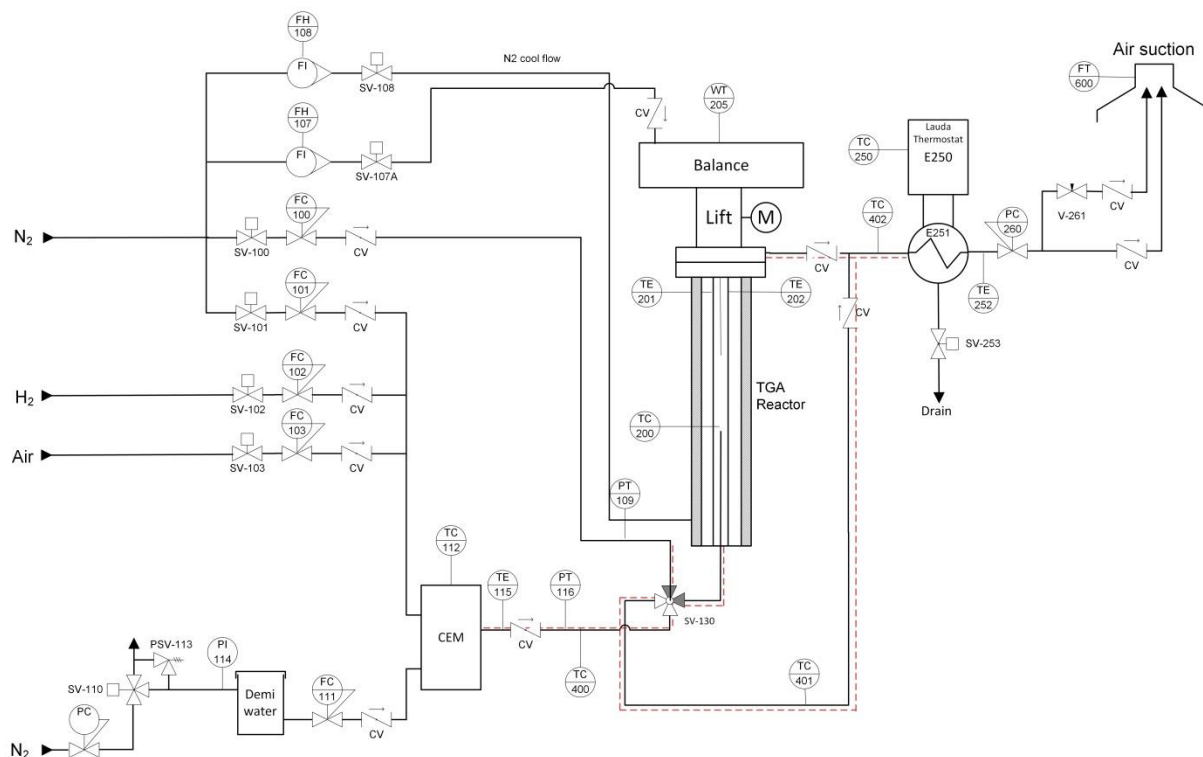
Fig.2. Schematic overview of the HPTGA at higher flow rates (HP_HF_TGA) used in this work.

2.2 Oxygen carrier characterization

The surface area and pore size distribution of all the oxygen carrier samples before and after the experiments were determined by the Brunauer-Emmett-Teller (BET) method by adsorption/desorption of nitrogen at 77 K in a Thermo-Scientific Surfer. The number of active sites were correlated with the probe molecule absorbed in static volumetric chemisorption with temperature programmed adsorption. A gas expansion pycnometer (Quantachrome Ultrapyc 1200e) has been used to measure the volume of a weighted sample of the solid carrier, from which the skeletal density can be calculated. This value is also used in the BET-method to determine the specific surface area. In addition, the microstructure of different samples was analysed in a FEI Quanta 3D FEG scanning electron microscope (SEM) to measure the difference in pore size and the distribution of the chemical elements in the oxygen carrier.

Crystalline species were identified by X-Ray Diffraction (XRD) in a Rigaku diffractometer at 298 K with a mobile Cu anode.

3 Results and Discussion

3.1 Study of the reactivity of the oxygen carrier at high pressures

The redox cycles were carried out in the three different TGAs with 15 min reduction (H_2, N_2), 10 min oxidation (100% Air) and constant partial pressure of H_2 of 1 bar, with different flow rates, different temperatures and different total pressures.

First, several redox cycles were carried out at different flow rates and 800 °C in the LPTGA at atmospheric pressure. From Fig.3 it can be concluded that no influence of mass transfer limitations was observed when operating at 1 bar with a total flow rate of at least 250 mL/min.
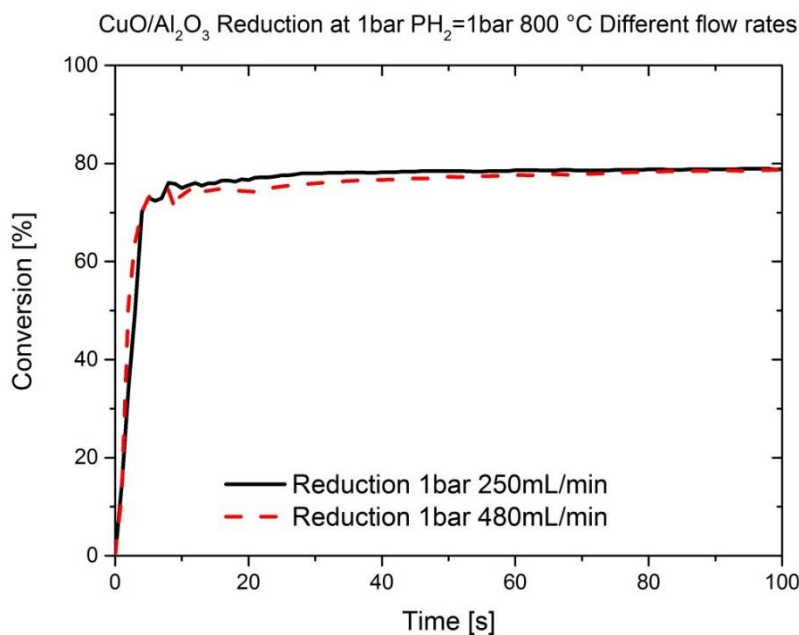

Fig.3. Reduction conversions at 1 bar, $PH_2 = 1$ bar and 800 °C in the LPTGA with different flow rates.

After assessing that mass transfer limitations should not play a role with a flow rate of 480 mL/min, an extensive study on the kinetics of CuO/Al_2O_3 at different operating pressures was carried out with the HPTGA from Rubotherm, where also the maximum flow rate available is 480 mL/min. In Fig.4 the reduction conversions are plotted for the experiments with a constant partial pressure of H_2 of 1 bar, at 800 °C, a total flow rate of 480 mL/min and different total pressures (the same sample was used for all the conditions in this experiment).
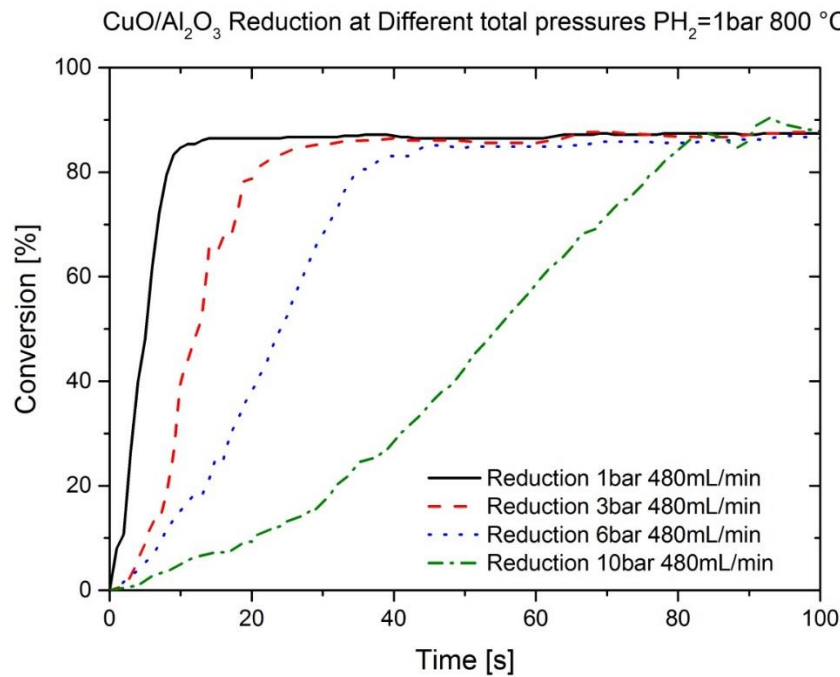

Fig.4. Reduction conversions at $PH_2 = 1$ bar, 800 °C and different total pressures in the HPTGA from Rubotherm.

A negative effect of the total pressure on the redox kinetics can clearly be observed in Figure 4, being more pronounced at higher pressures (10 bar). Because the partial pressure of H_2 was kept constant at 1 bar during all the experiments, it was not expected that the total pressure would have an effect on the redox kinetics. This negative effect of the pressure was also previously

observed by other researchers, but no physical explanation was provided [14–16,18–20], [22–26]. To assure that the reported pressure effect was not caused by the wrong gas velocities due to mass transfer limitations at higher pressures, the tests were repeated in the HP_TGA_HF.

First, a comparison between experiments at the same conditions in the different TGAs was performed to assure that the same kinetics were measured before starting the experiments with the HP_TGA_HF. This comparison is shown in Fig.5. The results of two TGAs are virtually identical and fully reproducible, indicating that the setups provide the same results when operated at the same conditions. From here all the results are carried out with the HP_TGA_HF, where higher pressures and higher flow rates are available.
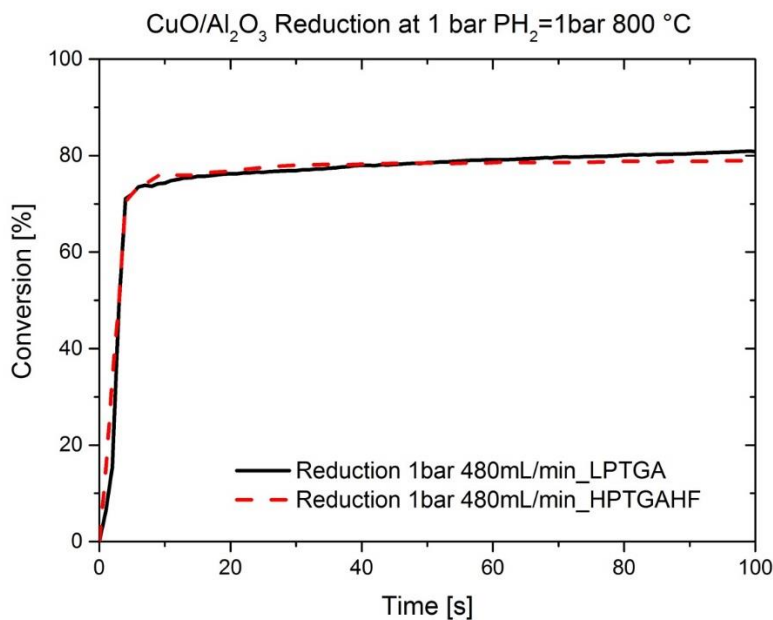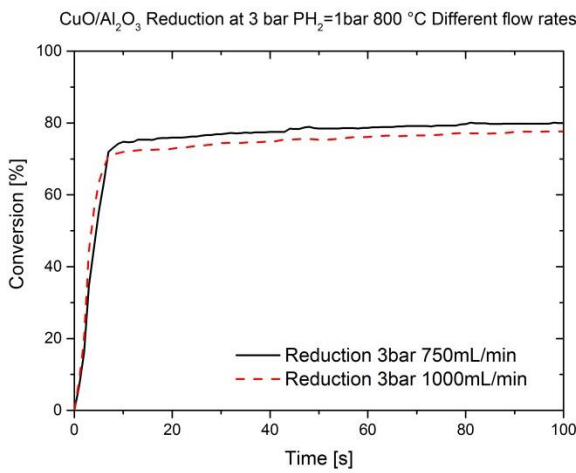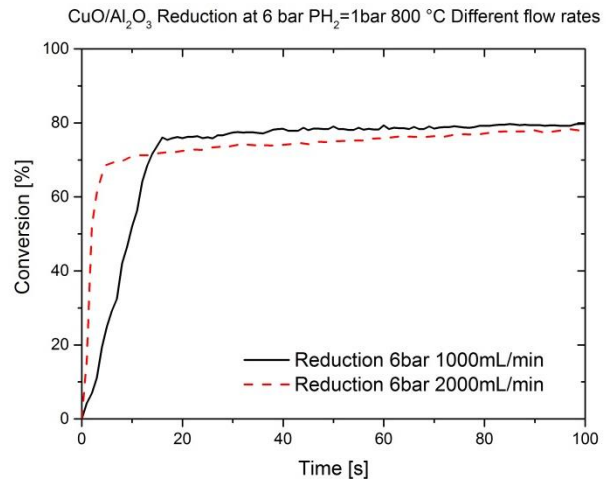

Fig.5. Reduction conversions at 1 bar, $PH_2 = 1$ bar, 800 °C and 480 mL/min for the LPTGA and the HP_TGA_HF.

Subsequently, experiments up to 2 L/min were performed at 3, 6 and 8 bar (since at 1 bar it was already proven that there were no mass transfer limitations at 250 and 480 mL/min). In Fig.6 the plots for the different total pressures at different flow rates are shown at 800 °C. (The same sample was used for all the conditions at one total pressure in these experiments).
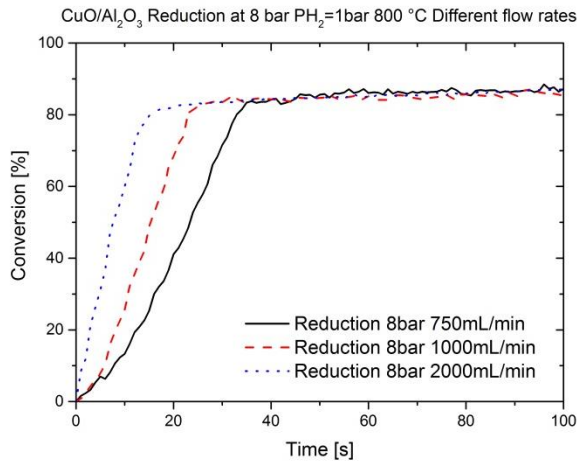
a)

b)

c)

Fig.6. Reduction conversions at $PH_2 = 1bar$, 800 °C and different flow rates and different total pressures: a) 3 bar, b) 6 bar and c) 8 bar.

At 3 bar total pressure no effects of mass transfer limitations are observed already for a flow rate of 1000 mL/min, while for 6 bar there is an effect of mass transfer limitations between 1 L/min and 2 L/min. At 8 bar effects of mass transfer limitations can be discerned even when using 2 L/min. The experiments at 6 and 8 bar were repeated increasing the flow rate (Therefore the gas velocity is also increased because it depends on the volumetric flow rate and the area of the reactor) up to the maximum flow rate available (6 L/min). At 3 bar the absence of mass transfer limitations was already shown when 1 L/min is used. The experimental results for 6 and 8 bar at higher flow rates are shown in Fig.7. (The same sample was used for all the conditions at one total pressure in these experiments).
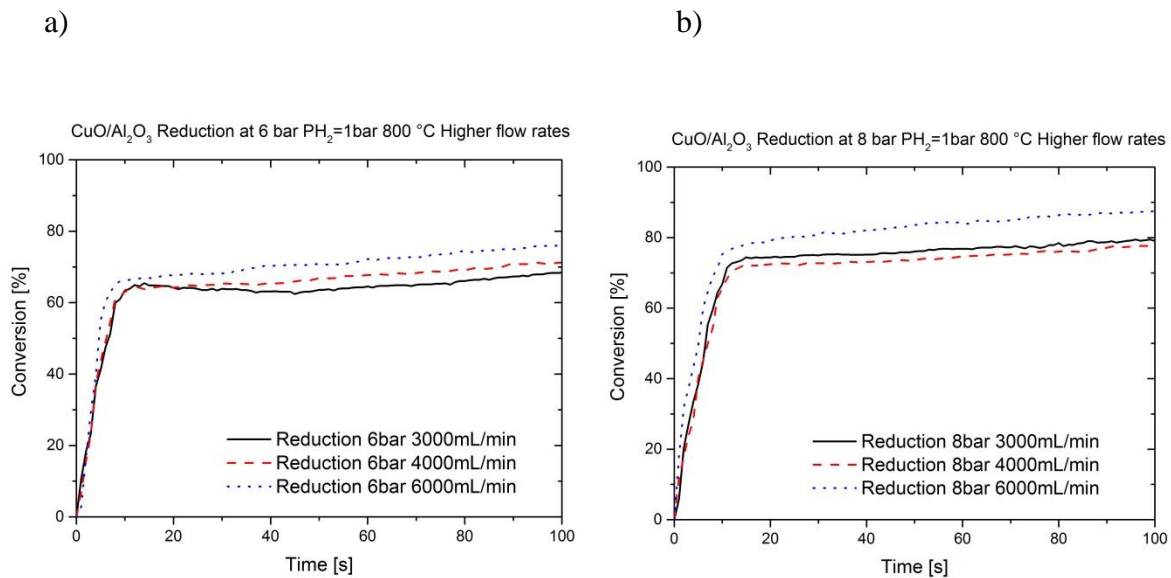
a)   b)

Fig.7. Reduction conversions at $PH_2 = 1$ bar, 800 °C and higher flow rates, a) 6 bar and b) 8 bar.

At 6 bar, the absence of mass transfer limitations is confirmed when the maximum flow rate, 6 L/min, is used, however, this flow rate is still insufficient to avoid mass transfer limitations when operating at 8 bar.

Fig.8 provides a comparison of the reduction conversions as a function of time for all the investigated pressures, using the necessary flow rates to avoid mass transfer limitations. The

temperature used was again 800 °C while the partial pressure of H_2 was kept constant at 1 bar. (The same sample was used for all the conditions in this experiment).
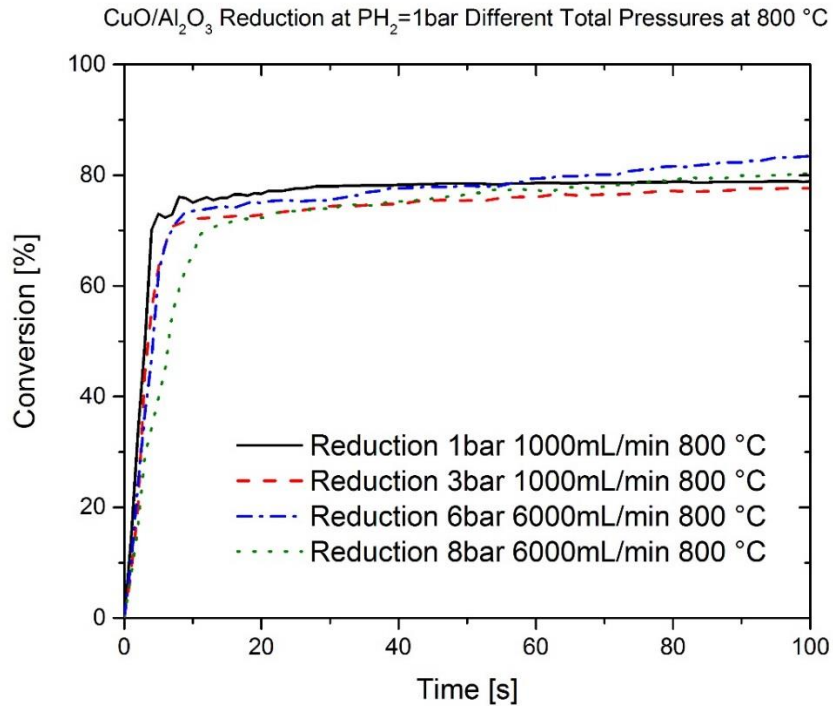

Fig.8. Reduction conversions at $PH_2 = 1$ bar, 800 °C and high flow rates for 1, 3, 6 and 8 bar of total pressure.

Fig.8 shows that the redox kinetics at a total pressure from 1 to 6 bar are the same for the same temperature and H_2 partial pressure, and that the negative effect of the total pressure on the kinetics is absent if sufficiently high flow rates (sufficiently gas velocities) are used to avoid mass transfer limitations. Clearly, the total pressure does not affect the redox kinetics if the partial pressure of H_2 is kept constant at 1 bar. At 8 bar, somewhat slower kinetics were observed, because it was not possible to reach even higher flow rates due to limitations of the setup. From these results it can be concluded that the cause of the negative effect of pressure of

the redox kinetics observed in other studies [14–16,18–20], [22–26], [30], [31], were possibly related to mass transfer limitations in the used set-ups. The influence of pressure on the redox kinetics at different temperatures is investigated next.

3.2 Study of the reactivity of the oxygen carrier at high pressures and different temperatures

Experiments at different temperatures while keeping the total pressure constant at 1, 3, 6 and 8 bar respectively, were carried out to study the influence of the temperature on the kinetics at higher pressures and the results are shown in Fig.9. (The same sample was used for all the conditions at one total pressure in these experiments).
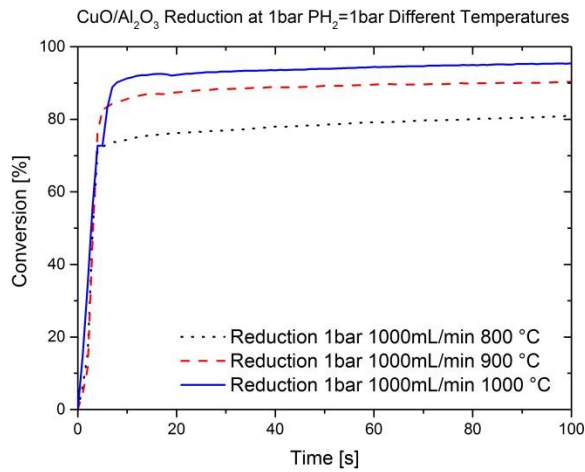
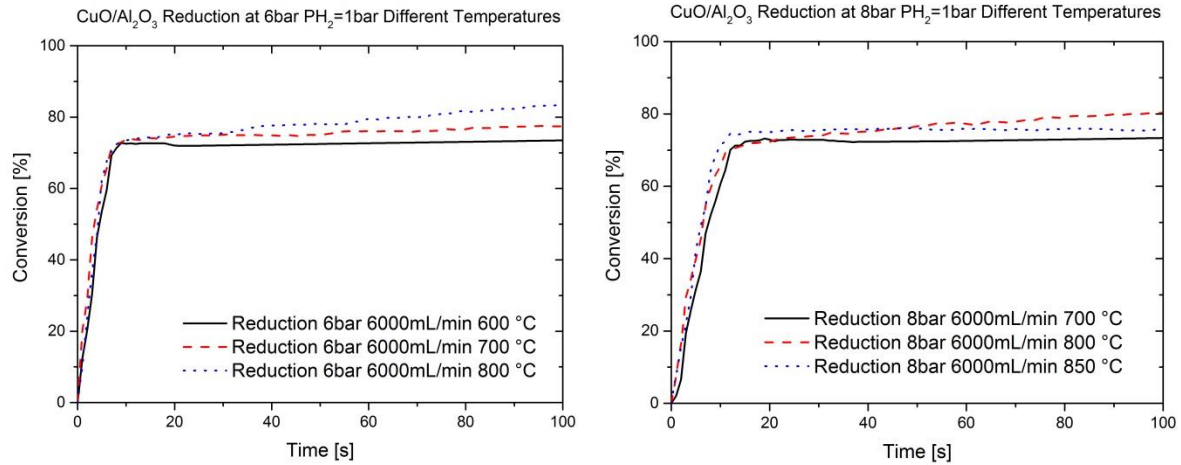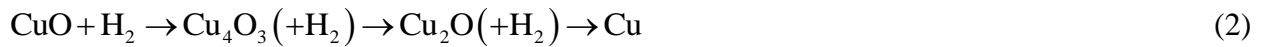a)   b)
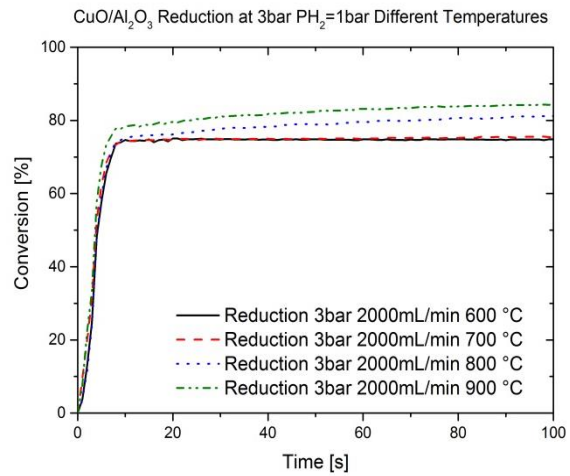
c)   d)

Fig.9. Reduction conversions at $PH_2 = 1$ bar, high flow rates and different temperatures for a) 1 bar, b) 3 bar, c) 6 bar and d) 8 bar of total pressure.

Fig.9 shows that the temperature does not influence the initial fast kinetics, which is virtually the same for all different temperatures and pressures investigated. This is consistent with the results obtained in a previous study on the kinetics of the same CuO/Al_2O_3 oxygen carrier at different temperatures and but at atmospheric pressure [24]. A sudden decrease in the rate of the reduction reaction is also clearly observed after a certain particle conversion (which is higher at higher temperatures) reaching a higher final conversion at higher temperatures. This drop observed in the reaction rate at around 70-80% particle conversion has been attributed to kinetic limitations in the reduction of $CuAl_2O_4$ (Eqs.(3)-(4)), which is favoured at higher temperatures [29], [24].

$$CuO + H_2 \rightarrow Cu_4O_3 (+H_2) \rightarrow Cu_2O(+H_2) \rightarrow Cu \tag{2}$$

$$CuAl_2O_4 + H_2 \rightarrow Cu + Al_2O_3 + H_2O \tag{3}$$

$$2CuAl_2O_4 + H_2 \rightarrow 2CuAlO_2 + Al_2O_3 + H_2O \tag{4}$$

XRD was performed after reduction at different temperatures, where it was observed that there is a smaller amount of spinel at higher temperatures (the XRD patterns are provided in the supplementary material), which explains why the sudden decrease in the reduction rate takes place at higher particle conversions when operating at higher temperatures, because more $CuAl_2O_4$ has been converted to Cu and $CuAlO_2$ (Eqs. (3)-(4)). In Fig.8 the TGA results for operation at different total pressures at 800 °C were plotted, observing the same final conversion and the same kinetics independent of the total pressure used, except for the experiment at 8 bar, where external mass transfer limitations still play a role. This can also be observed from Fig.10 where the TGA results for different total pressures are plotted at 700 °C. (The same sample was used for all the conditions in this experiment).
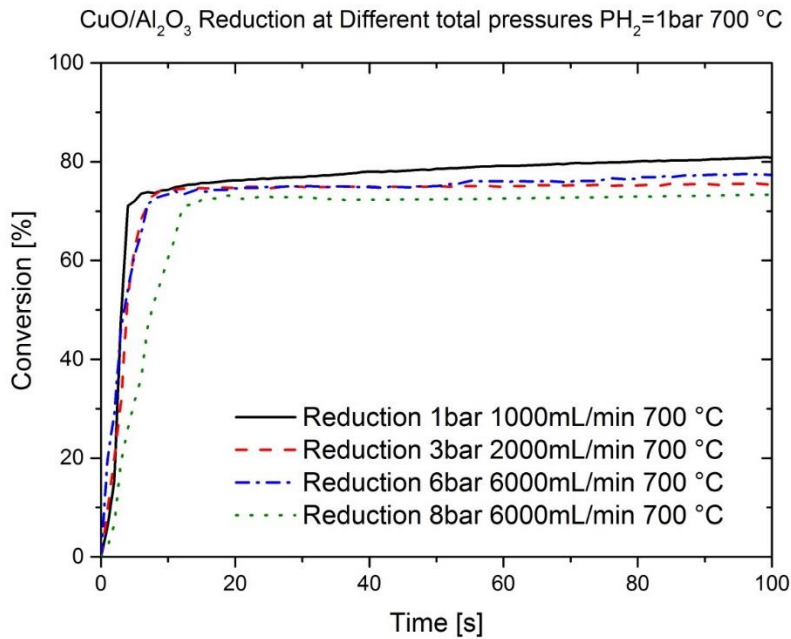

Fig.10. Reduction conversions at $PH_2 = 1$ bar, 700 °C and high flow rates for 1, 3, 6 and 8 bar of total pressure.

In a previous study [29], the absence of internal mass transfer limitations inside the particle was proven. In Fig.11 the TGA results for the crushed particles are compared with the TGA results with the standard particles of 1.1 mm diameter to study the effect of internal mass transfer limitations inside the particles. The redox cycles were carried out in both cases under a total pressure of 3 bar, partial pressure of hydrogen 1 bar, and a high flow rate of 2000 mL/min to avoid external mass transfer limitations at a temperature of 800 °C. It can be concluded that internal mass transfer limitations inside the particle can be neglected for this oxygen carrier, CuO/Al_2O_3. It has been observed in other oxygen carriers that internal diffusion becomes important once particle size exceeds 2 mm [10], so in this case it can be due to smaller particles used of 1.1 mm diameter.
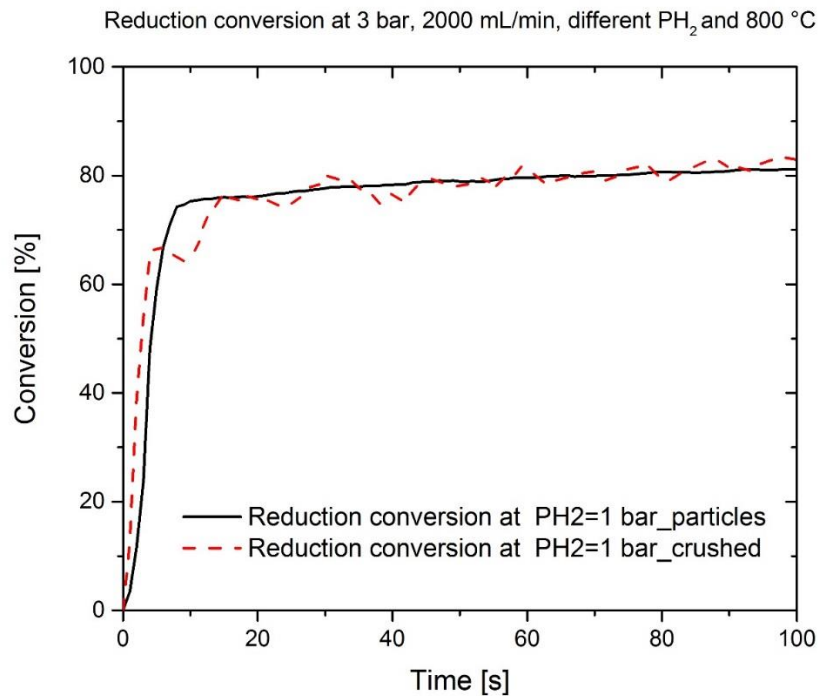

Fig.11. Reduction conversions at 3 bar of total pressure, flow rate of 2000 mL/min, PH_2 of 1 bar and 800 °C for particles and powder.

To investigate if the absence of internal mass transfer limitations inside the particle [29] occurs also at high pressures, to investigate the effect of PH_2 on the redox kinetics, several redox cycles were carried out under the same conditions (total pressure of 3 bar and different partial pressures of hydrogen) for crushed particles with a particle size distribution of between 0.5 and 478 µm. (The same sample was used for all the conditions in this experiment).

Fig.12 shows that the PH_2 has a negligible effect on the redox kinetics. A possible explanation is that H_2 does not diffuse through the particle grain, but is reacting very fast on the grain surface imposing a virtually zero oxygen concentration at the grain surface. The redox kinetics is then determined by the oxygen diffusion through the grain and does not depend on the H_2 partial pressure. This also suggests that varying the total pressure, and keeping the partial pressure of H_2 constant, without compensating for the fuel partial pressure, there is also no effect on conversion [30].
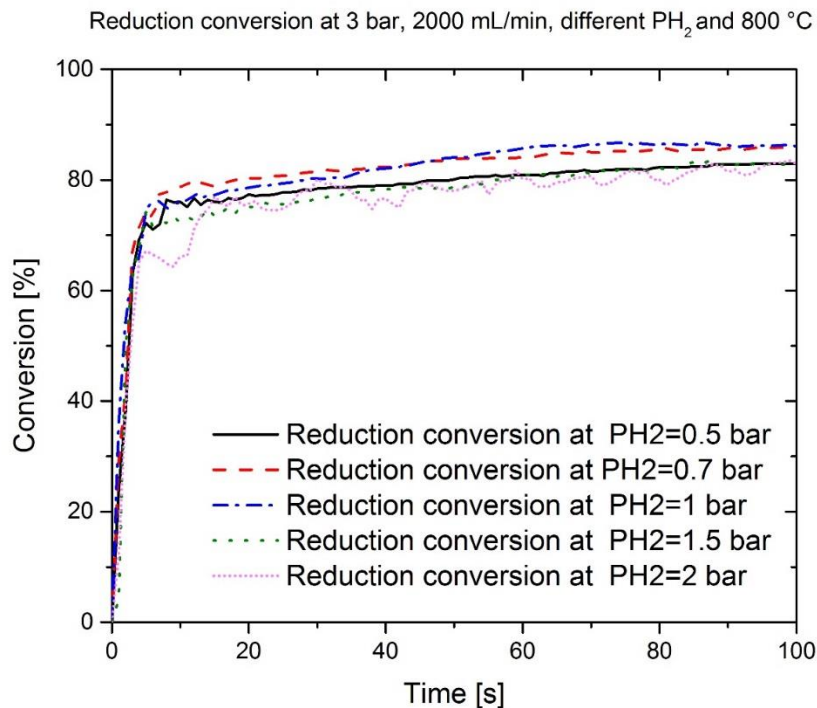
Fig.12. Reduction conversions at 3 bar of total pressure, flow rate of 2000 mL/min and different PH$_2$ at 800 °C.

3.3 Study of the morphology of the oxygen carrier at different pressures and different temperatures

The BET surface area and mean pore radius was determined at the end of the reduction cycle for the TGA experiments carried out at different total pressures (see Table 1, the BET isotherms are provided in the supplementary material).

Table 1. BET results after reduction of CuO/Al$_2$O$_3$ at 800 °C and 1, 3, 6 and 10 bar.

Experiment	Mean pore radius [nm]	Surface area [m^2/g]

CuO/Al$_2$O$_3$ Reduction 1bar	2.1897	8.0853
PH2 = 1 bar 800 °C		
CuO/Al$_2$O$_3$ Reduction 3bar	2.5625	7.5138
PH2 = 1 bar 800 °C		
CuO/Al$_2$O$_3$ Reduction 6bar	1.8276	8.2062
PH2 = 1 bar 800 °C		
CuO/Al$_2$O$_3$ Reduction 10bar	2.1664	7.8798
PH2 = 1 bar 800 °C		

Table 1 shows that no significant change in the surface area as well as in the mean pore radius is observed for the TGA experiments at different pressures. The absence of an effect of the total pressure on the morphology of the oxygen carrier corresponds to the absence of influence of pressure on the redox kinetics, contrary to what Chauk et al. [13] observed, indicating that the sulfidation conversion was adversely affected by increasing pressure as a result of CaO sorbent morphological alterations, such as reduction in surface area. This can be due to the use of a different oxygen carrier and therefore, its preparation.

SEM images were taken after the reduction reactions at 800 °C and different total pressures while keeping the partial pressure of H$_2$ constant at 1 bar and are shown in Fig.13. Also the SEM images confirm that there are no differences in the micro-structure when the pressure during the reduction is increased from 1 to 10 bar, and that the operation at higher pressures does not incur the formation of bigger cracks or void fraction.
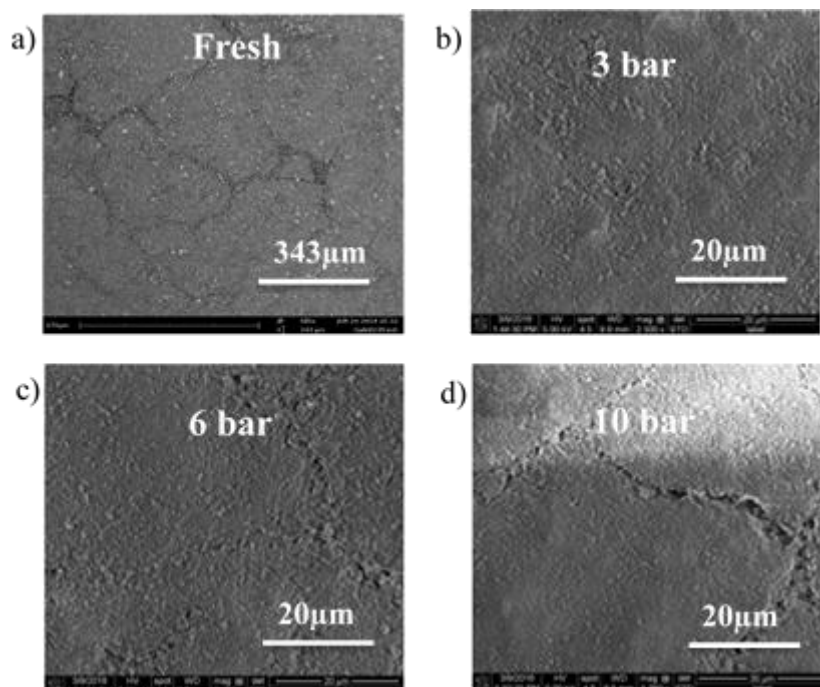
Fig.13. SEM images for reduction of CuO/Al_2O_3 at 800 °C, $PH_2 = 1$ bar, a) fresh, b) 1 bar, c) 3 bar and d) 8 bar.

Finally, XRD was performed on the samples operated at different total pressures at 800 °C. In Fig.14 all the patterns for the samples operated at different pressures are shown together, and clearly show the same pattern, indicating that there is no difference in the chemical phases. These results were also expected on the basis of the results shown in Fig.8 and Fig.10, which showed that the drop in the reduction rate and the final conversion at the same temperature are the same independent of the total pressure.
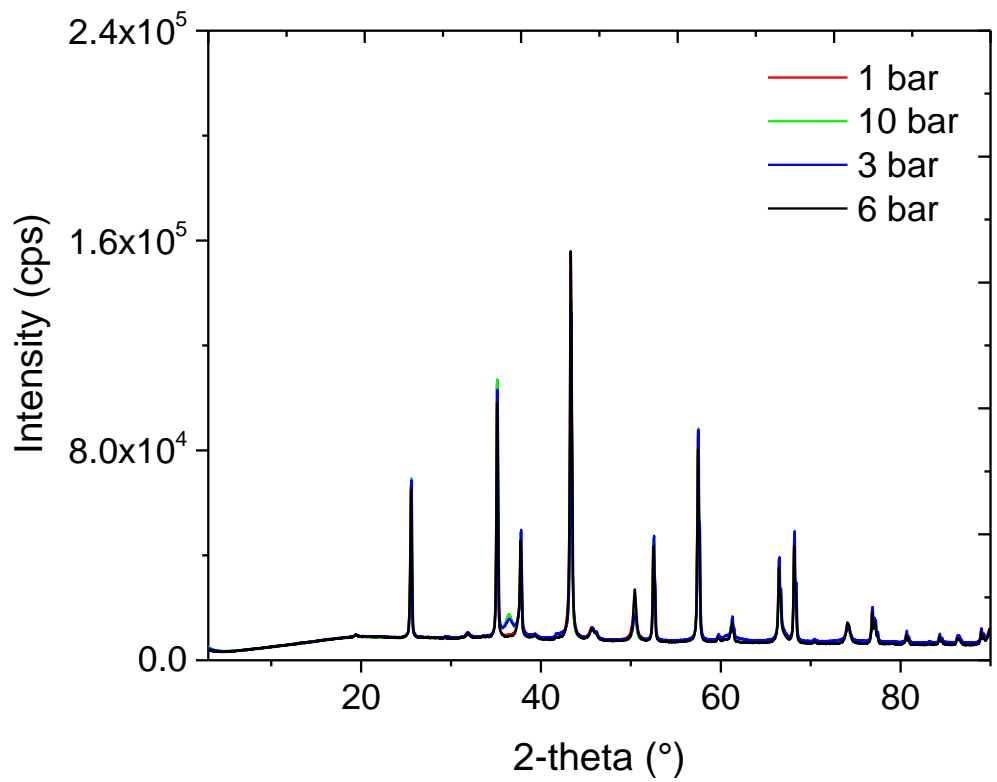
Fig. 14. XRD pattern for CuO/Al$_2$O$_3$ reduction at 800 °C, PH$_2$ = 1 bar and different total pressures.

4   Conclusions

TGA experiments have been carried out on a CuO/Al_2O_3 oxygen carrier using three different TGA setups allowing operation under different operating pressures and gas flow rates in order to elucidate the effect of the total pressure on the redox kinetics. Based on the results shown in this study, it is possible to conclude that the negative effect of the total pressure on the redox kinetics of oxygen carriers previously reported in literature was most probably caused by external mass transfer limitations rather than physical effects of the pressure on the micro-kinetics. Influence of external mass transfer limitations can be avoided by using higher total gas flow rates, where even higher flow rates are required when operating at higher pressures. No effect of the total pressure on the redox kinetics has been found, and also no differences in the micro-structure and chemical phases were detected when the redox cycles were performed at different total pressures. The initial reduction kinetics was very fast and independent of temperature and pressure, but the sudden decrease in the reduction rate takes place at higher particle conversions when the reduction is carried out at higher temperatures. The initial kinetics of the reduction reaction are very fast up to the first 20 s, where CuO is converted to Cu, and $CuAl_2O_4$ is reduced to Cu, where this last reaction is favoured at higher temperatures, explaining the increase in conversion at which the sudden decrease in the reduction rate takes place when operating at higher temperatures.

5 References

[1]   A.A. Olajire, CO2 capture and separation technologies for end-of-pipe applications – A review, Energy. 35 (2010) 2610–2628. doi:10.1016/j.energy.2010.02.030.

[2]   J. Wilcox, Global climate and energy project, (n.d.). https://gcep.stanford.edu/pdfs/2wh9Q1Alh3q2zMOQRKD4MQ/JenWilcox_CarbonCapture101_web.pdf (accessed March 28, 2014).

[3]   J. Davison, Performance and costs of power plants with capture and storage of CO2, Energy. 32 (2007) 1163–1176. doi:10.1016/j.energy.2006.07.039.

[4]   K. Tan, Y; Thambimuthu, OXY-fuel Combustion at the CANMET Vertical Combustor Research Faciltiy - 4b2.pdf, (n.d.). http://seca.doe.gov/publications/proceedings/01/carbon_seq/4b2.pdf (accessed March 28, 2014).

[5]   B.J.P. Buhre, L.K. Elliott, C.D. Sheng, R.P. Gupta, T.F. Wall, Oxy-fuel combustion technology for coal-fired power generation, Prog. Energy Combust. Sci. 31 (2005) 283–307. doi:10.1016/j.pecs.2005.07.001.

[6]   F.H.. Peron, CO2 capture processes and costs, (n.d.). http://ogst.ifpenergiesnouvelles.fr/articles/ogst/pdf/2005/03/feron1_vol60n3.pdf (accessed March 28, 2014).

[7]   T. Wall, Y. Liu, C. Spero, L. Elliott, S. Khare, R. Rathnam, F. Zeenathal, B. Moghtaderi, B. Buhre, C. Sheng, R. Gupta, T. Yamada, K. Makino, J. Yu, An overview on oxyfuel coal combustion—State of the art research and technology development, Chem. Eng. Res. Des. 87 (2009) 1003–1016. doi:10.1016/j.cherd.2009.02.005.

[8]   D.Y.C. Leung, G. Caramanna, M.M. Maroto-Valer, An overview of current status of carbon dioxide capture and storage technologies, Renew. Sustain. Energy Rev. 39 (2014) 426–443. doi:10.1016/j.rser.2014.07.093.

[9]   J. Wolf, M. Anheden, J. Yan, Comparison of nickel- and iron-based oxygen carriers in chemical looping combustion for CO capture in power generation, Fuel. 84 (2005) 993–1006. doi:10.1016/j.fuel.2004.12.016.

[10]   O. Nordness, L. Han, Z. Zhou, G.M. Bollas, High-Pressure Chemical-Looping of Methane and Synthesis Gas with Ni and Cu Oxygen Carriers, (2015).

[11]   S. Noorman, M. van Sint Annaland, Packed Bed Reactor Technology for Chemical-Looping Combustion, Ind. Eng. Chem. Res. 46 (2007) 4212–4220. doi:10.1021/ie061178i.

[12]   V. Spallina, M.C. Romano, P. Chiesa, F. Gallucci, M. van Sint Annaland, G. Lozza, Integration of coal gasification and packed bed CLC for high efficiency and near-zero emission power generation, Int. J. Greenh. Gas Control. 27 (2014) 28–41. doi:10.1016/j.ijggc.2014.04.029.

[13]   S.S. Chauk, R. Agnihotri, R.A. Jadhav, S.K. Misro, L.-S. Fan, Kinetics of high-pressure removal of hydrogen sulfide using calcium oxide powder, AIChE J. 46 (2000) 1157–1167. doi:10.1002/aic.690460608.

[14]   Rajeev Agnihotri, Suhas K. Mahuli, and Shriniwas S. Chauk, L.-S. Fan*, Influence of Surface Modifiers on the Structure of Precipitated Calcium Carbonate, (1999). doi:10.1021/IE9900521.

[15]   R. Agnihotri, S.S. Chauk, S.K. Misro, L.-S. Fan, High-Pressure Reaction Kinetics of

Hydrogen Sulfide and Uncalcined Limestone Powder, Ind. Eng. Chem. Res. 38 (1999) 3802–3811. doi:10.1021/ie990271m.

[16]   K. Qiu, E.J. Anthony, L. Jia, Oxidation of sulfided limestone under the conditions of pressurized fluidized bed combustion, Fuel. 80 (2001) 549–558. doi:10.1016/S0016-2361(00)00128-9.

[17]   F. Garcia-Labiano, J. Adanez, A. Abad, Effect of pressure on the behavior of Copper-, Iron-and Nickel-based Oxygen Carriers for Chemical Looping Combustion, Energy&Fuels. 20 (2006) 26–33.

[18]   S.K.. F. Agnihotri, R.; Chauk, S. S.; Misro, Effect of Pressure on the Sulfidation of Calcined-Based Sorbents, Chem.Res. 38 (1999) 3802–3811.

[19]   L. Chauk, SS; Agnihotri, R; Jadhav, RA; Misro, SK; Fan, Kinetics of high-pressure removal of hydrogen sulfide using calcium oxide powder, AICHE J. 46 (2000) 1157–1167.

[20]   A. Abad, F. García-Labiano, L.F. de Diego, P. Gayán, J. Adánez, Reduction Kinetics of Cu-, Ni-, and Fe-Based Oxygen Carriers Using Syngas (CO + H 2) for Chemical-Looping Combustion, Energy & Fuels. 21 (2007) 1843–1853. doi:10.1021/ef070025k.

[21]   L.F. de Diego, F. García-Labiano, J. Adánez, P. Gayán, A. Abad, B.M. Corbella, J. María Palacios, Development of Cu-based oxygen carriers for chemical-looping combustion, Fuel. 83 (2004) 1749–1757. doi:10.1016/j.fuel.2004.03.003.

[22]   J.Y. Kim, J.A. Rodriguez, J.C. Hanson, A.I. Frenkel, P.L. Lee, Reduction of CuO and Cu2O with H2: H embedding and kinetic effects in the formation of suboxides., J. Am. Chem. Soc. 125 (2003) 10684–92. doi:10.1021/ja0301673.

[23] L.F. De Diego, J. Ada, A. Abad, P. Gaya, M.L. Casta, Reduction and Oxidation Kinetics of a Copper-Based Oxygen Carrier Prepared by Impregnation for Chemical-Looping Combustion, (2004) 8168–8177.

[24] E.M. Eyring, G. Konya, J.S. Lighty, a. H. Sahir, a. F. Sarofim, K. Whitty, Chemical Looping with Copper Oxide as Carrier and Coal as Fuel, Oil Gas Sci. Technol. – Rev. d'IFP Energies Nouv. 66 (2011) 209–221. doi:10.2516/ogst/2010028.

[25] M.M. Hossain, H.I. de Lasa, Chemical-looping combustion (CLC) for inherent separations—a review, Chem. Eng. Sci. 63 (2008) 4433–4451. doi:10.1016/j.ces.2008.05.028.

[26] K. Wang, Q. Yu, Q. Qin, Reduction Kinetics of Cu-Based Oxygen Carriers for Chemical Looping Air Separation, (2013).

[27] K. Coenen, F. Gallucci, P. Cobden, E. van Dijk, E. Hensen, M. van Sint Annaland, Chemisorption working capacity and kinetics of CO_2 and H_2O of hydrotalcite-based adsorbents for sorption-enhanced water-gas-shift applications, Chem. Eng. J. 293 (2016) 9–23. doi:10.1016/j.cej.2016.02.050.

[28] H.P. Hamers, F. Gallucci, G. Williams, P.D. Cobden, M. van Sint Annaland, Reactivity of Oxygen Carriers for Chemical-Looping Combustion in Packed Bed Reactors under Pressurized Conditions, Energy & Fuels. 29 (2015) 2656–2663. doi:10.1021/ef5027899.

[29] M.A. San Pio, I. Roghair, F. Gallucci, M. van Sint Annaland, Investigation on the decrease in the reduction rate of oxygen carriers for chemical looping combustion, Powder Technol. 301 (2016) 429–439. doi:10.1016/j.powtec.2016.06.031.

[30] I. Adánez-Rubio, P. Gayán, A. Abad, F. García-Labiano, L.F. de Diego, J. Adánez,